AD-A259 936

HDL-TR-2202

September 1992

Processing of Patterned Ferroelectric Capacitors

by Bernard J. Rod

DTIC
ELECTE
JAN 2 1 1993
S B D
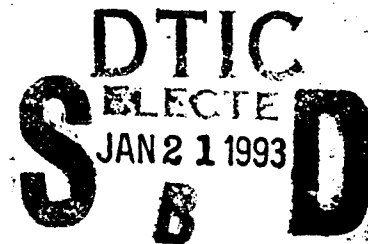
U.S. Army Research Laboratory
Harry Diamond Laboratories
Adelphi, MD 20783-1197

93 1 19 019

REPORT DOCUMENTATION PAGE

Public reporting burden for this collection of information is estimated to average 1 hour per response, including the time for reviewing instructions, searching existing data sources, gathering and maintaining the data needed, and completing and reviewing the collection of information. Send comments regarding this burden estimate or any other aspect of this collection of information, including suggestions for reducing this burden, to Washington Headquarters Services, Directorate for Information Operations and Reports, 1215 Jefferson Davis Highway, Suite 1204, Arlington, VA 22202-4302, and to the Office of Management and Budget, Paperwork Reduction Project (0704-0188), Washington, DC 20503

1. AGENCY USE ONLY *(Leave blank)*	2. REPORT DATE September 1992	3. REPORT TYPE AND DATES COVERED Final, from January 1991 to September 1991

4. TITLE AND SUBTITLE

Processing of Patterned Ferroelectric Capacitors

5. FUNDING NUMBERS

PE: 62120

6. AUTHOR(S)

Bernard J. Rod

7. PERFORMING ORGANIZATION NAME(S) AND ADDRESS(ES)

Harry Diamond Laboratories
2800 Powder Mill Road
Adelphi, MD 20783-1197

8. PERFORMING ORGANIZATION REPORT NUMBER

9. SPONSORING/MONITORING AGENCY NAME(S) AND ADDRESS(ES)

U.S. Army Research Laboratory
2800 Powder Mill Road
Adelphi, MD 20783-1145

10. SPONSORING/MONITORING AGENCY REPORT NUMBER

11. SUPPLEMENTARY NOTES

AMS code: 612120.H250011
HDL PR: 1XE723

12a. DISTRIBUTION/AVAILABILITY STATEMENT

Approved for public release; distribution unlimited.

12b. DISTRIBUTION CODE

13. ABSTRACT *(Maximum 200 words)*

Processing steps are described in detail for a procedure to fabricate sol-gel-derived lead-zirconate-titanate (PZT) ferroelectric thin-film capacitors in a manner compatible with processed complementary metal-oxide-semiconductor (CMOS) integrated-circuit wafers. The intended purpose of this work is to fabricate nonvolatile-element memory test structures for electrical and radiation characterization studies. A number of critical processing issues dealing with the etching of the PZT films and the deposition and definition of the top and bottom platinum electrodes were addressed and suitable solutions found during the course of this work. Using the procedures described herein, we fabricated working PZT capacitors and evaluated them electrically.

14. SUBJECT TERMS

Ferroelectric capacitor, PZT, sputter etching

15. NUMBER OF PAGES
27

16. PRICE CODE

17. SECURITY CLASSIFICATION OF REPORT Unclassified	18. SECURITY CLASSIFICATION OF THIS PAGE Unclassified	17. SECURITY CLASSIFICATION OF ABSTRACT Unclassified	20 LIMITATION OF ABSTRACT UL

I

Contents

Page

Figures

Table

3   ᐟᵉˢ

r

A-1

1. Introduction

During the last few years, considerable interest has been rekindled in the application of ferroelectric materials to fabricate nonvolatile random-access memories (RAMs) that use a ferroelectric capacitor as the basic memory storage element [1–3]. Ferroelectric memories could be expected to be superior to memories based on standard technologies, not only because of their nonvolatility but also because the ferroelectric capacitor memory element itself is inherently radiation hard. In addition, because the dielectric constant of the ferroelectric material is considerably higher than that of silicon dioxide, the capacitor elements can be made much smaller than in conventional silicon-dioxide-based circuitry, and thus a significant increase in circuit component density and speed is a very real possibility. These advantages could be of considerable importance to advanced military ground and space-based electronics systems.

This report discusses a procedure developed to fabricate lead-zirconate-titanate (PZT) thin-film ferroelectric capacitors in a manner compatible with complementary metal-oxide semiconductor (CMOS) processed integrated circuits in order to produce memory element test chips; the resulting chips can be used for electrical and radiation characterization studies for the development of nonvolatile memory circuits. Figure 1 shows the basic ferroelectric capacitor structure and figure 2 shows a simplified schematic of a single memory element. The critical process steps needed to fabricate this device are the deposition and etching of the PZT films and the deposition and etching of the platinum top and bottom electrodes.

Figure 1. Ferroelectric capacitor cross section.
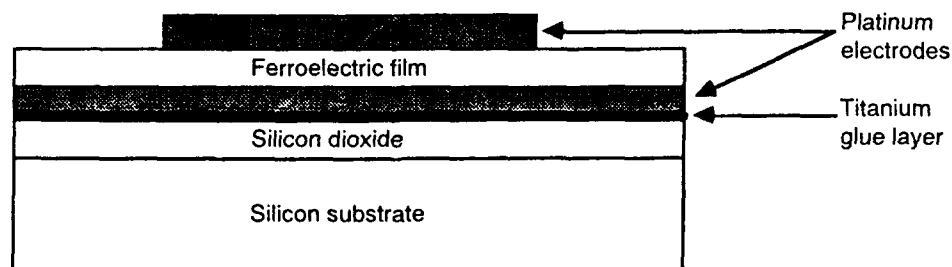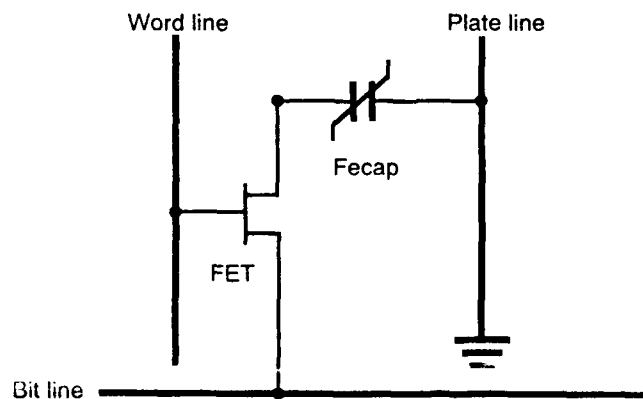

**Figure 2. Memory element schematic.**

Any number of different approaches can be taken to fabricate a working ferroelectric capacitor as an independent device in itself. However, when the capacitor is to be incorporated onto a wafer with existing CMOS integrated circuitry, a number of constraints are necessarily placed on its fabrication. Some of the concerns that must be adequately addressed in producing a CMOS-compatible ferroelectric memory element are the effects of high temperatures after integrated circuit processing, exposure to potentially contaminating substances, and removal or chemical attacking of the underlying circuitry by the processing chemicals. Thus, the critical process development issue to be addressed is the compatibility of the ferroelectric capacitor process with the underlying CMOS circuitry.

All the work discussed herein is based on the processing of PZT ferroelectric films deposited by the sol-gel process [4–5]. The sol-gel and hydrolyzing solutions used during the course of this work were obtained from outside sources, but the film depositions and annealing were done in our laboratory at Harry Diamond Laboratories (HDL). The actual sol-gel deposition process itself is not considered here since this will be the subject of a separate report. Furthermore, the PZT film may be deposited in a number of different ways and, other than minor differences in the etching times due to different film thicknesses and densities, there would be no effect on the subsequent processing sequence to be discussed here.

2. Mask Set

A mask set was generated to provide devices suitable for the process development work. Two basic capacitor structures employing a 40- × 40-µm and an 80- × 80-µm square-top platinum electrode were designed for this work. In part, these sizes were designed to permit the structure to be probed directly using a standard wafer probe station. The 80- × 80-µm device should also be large enough for wire bonding using a properly adjusted ball bonder. The mask levels provide for the etching of the top and bottom electrodes and the PZT island. For this initial effort, the PZT island was designed to be considerably larger than the top electrode. This design was intentional because it was not known just how much undercutting of the PZT would occur during the etching process, and this was one of the issues to be examined in this work. In an actual device intended for a memory element in an integrated circuit, the PZT island border need only be large enough to prevent shorting between the top and bottom electrodes. Although the actual sizes of the capacitors fabricated here are larger than what would be required for an integrated circuit memory element, the basic structure is the same. Figure 3 shows a composite of the three levels used in this work.

Figure 3. Composite of mask levels.

Platinum electrodes

PZT islands

Substrate contacts
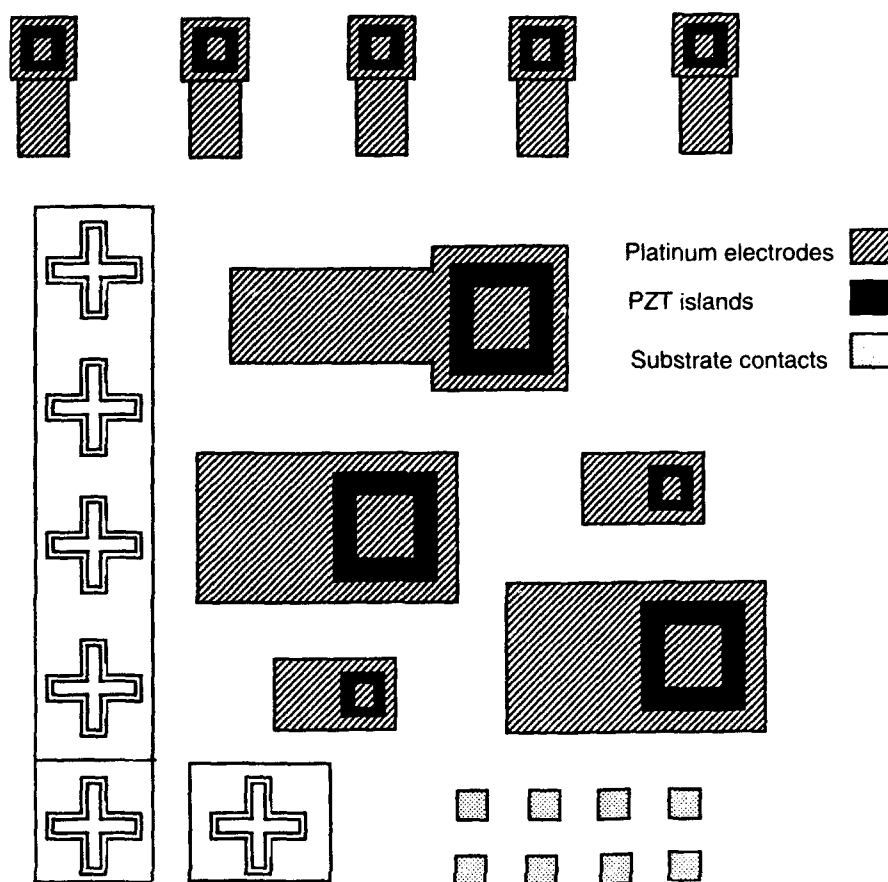
3. Photoresist Processing

Standard photoresist procedures were used to pattern the platinum and PZT during the fabrication of the capacitors, but with some modifications to the exposure and development times as discussed below. We used KTI 820 dyed and undyed photoresists with generally very acceptable results for all the work discussed here. The resist was spun onto the wafers at 5000 rpm and then soft-baked in an air oven at 105°C for 30 min. This procedure results in a photoresist film about 1.2 μm thick. An Optometrix 8010 wafer stepper employing a multi-frequency light source and G-line filter was used to expose the photoresist. For the PZT islands, undyed resist was used with a 2.5-s exposure. For the platinum levels, the dyed resist was used, and it was found that the exposure time had to be increased to 5 s or even longer to permit adequate exposure of the resist. This additional exposure time is believed to be caused by the strong internal reflections in the resist from high reflectivity of the underlying platinum.

Following the exposure, the resist was developed in KTI 934 100-percent positive photoresist developer diluted 1:1 with deionized water. Although

the recommended development time was 30 s, we found that on occasion it was necessary to increase this to as much as 50 s to adequately develop out the patterns on the highly reflective platinum surface. We did not observe any problems with the developed images as a result of the increased development times. Increasing the exposure even more could possibly reduce the development times, but this might also lead to overexposure of the pattern. Visually, the longer development times did not adversely affect the developed patterns. After developing the photoresist, a standard hard-bake in an air oven at 140°C for 30 min was used to remove any remaining solvents from the resist and harden it. However, we found that a longer bake time of up to 40 min was desirable to additionally harden the resist before any sputter etching.

Finally, the wafers were placed in an oxygen plasma asher for 15 to 30 s at 300 W, to remove any remaining photoresist film in the areas to be etched. The removal of this film is especially important when employing wet etching procedures because even a very thin film of photoresist can prevent the intended etching action from occurring. Some patterned photoresist loss does occur during the oxygen plasma ashing process, but this loss is not significant. This plasma ashing step was usually omitted when sputter etching was employed since the sputtering would quickly remove any remaining thin photoresist film in the areas to be etched.

4. Capacitor Process Sequence

Figure 4 shows the overall processing sequence. The starting material consisted of 4-in.-diam <100> silicon wafers of varying resistivity that had been cleaned using standard wafer cleaning procedures and then thermally oxidized using either dry or wet oxidation processes to produce oxide layers several hundred to a few thousand angstroms thick. The actual oxide thickness was not considered critical to this work, and oxidations were performed in whichever furnace tube was available at the time.

Following oxidation, the wafers were placed in a Materials Research Corporation (MRC) multitarget sputtering system for the bottom electrode deposition. This deposition consists of a titanium glue layer about 300 Å thick followed immediately, and without breaking vacuum, by a platinum layer about 1700 to 3000 Å thick. Before the deposition, we pumped the sputtering system down to a pressure of 4×10^{-4} Pa. A 2-min pre-sputter against the shutter cleaned the target before we sputter-deposited the appropriate metal. Power levels of 125 and 60 W into 5-in.-diam targets were used for the titanium and platinum, respectively. These sputtering conditions resulted in deposition rates of about 50 Å/min for the titanium and 200 Å/min for the platinum.

At this point the substrates were ready for the ferroelectric film to be applied. Figure 5 shows the procedure we used to apply the PZT films in our laboratory. Film thicknesses resulting from this procedure ranged from
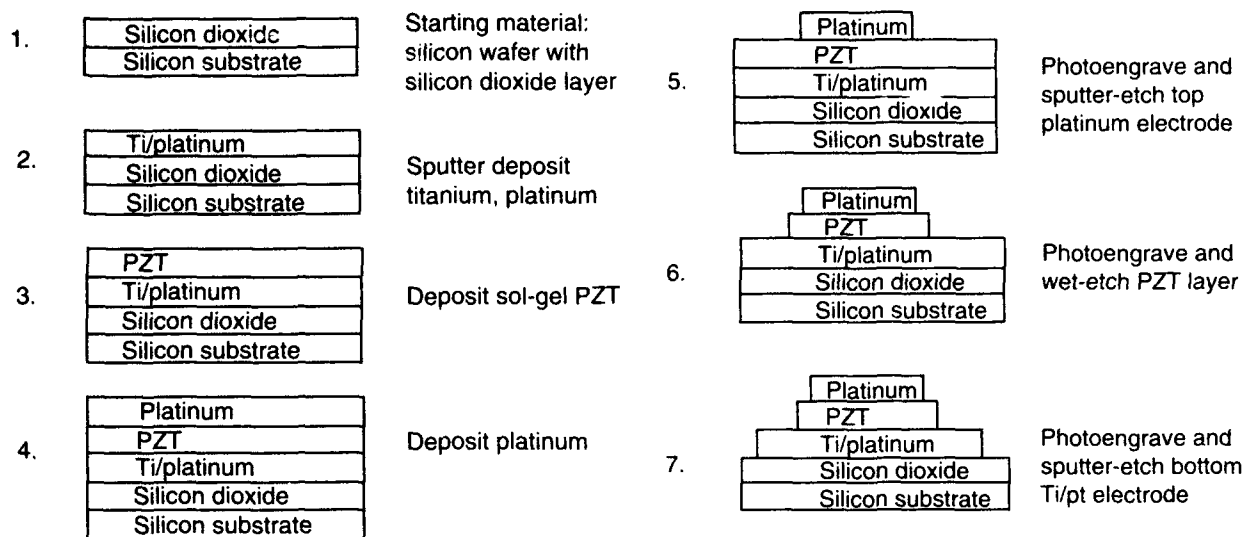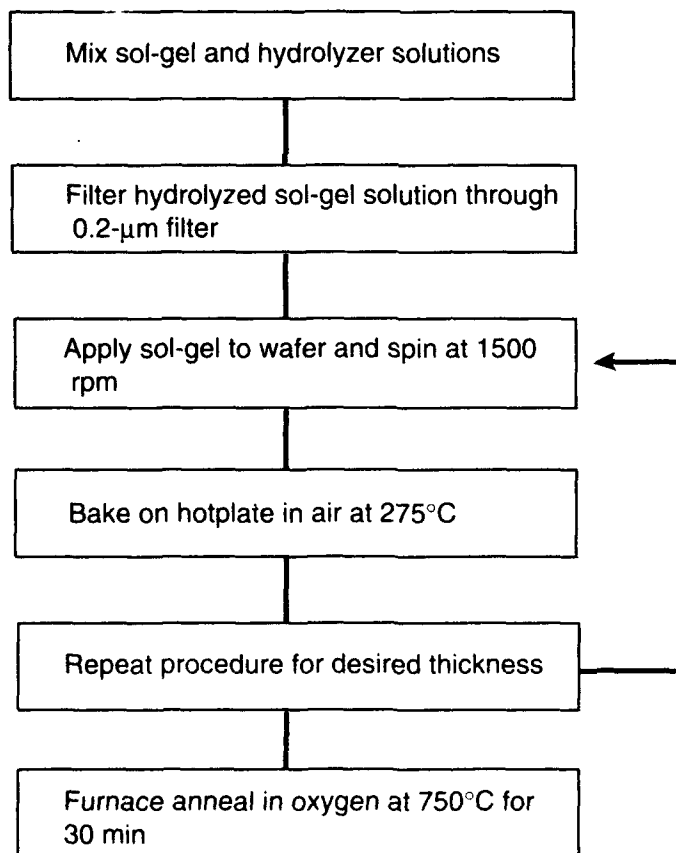
1.	Silicon dioxide
	Silicon substrate

Starting material: silicon wafer with silicon dioxide layer

2.	Ti/platinum
	Silicon dioxide
	Silicon substrate

Sputter deposit titanium, platinum

3.	PZT
	Ti/platinum
	Silicon dioxide
	Silicon substrate

Deposit sol-gel PZT

4.	Platinum
	PZT
	Ti/platinum
	Silicon dioxide
	Silicon substrate

Deposit platinum

5.	Platinum
	PZT
	Ti/platinum
	Silicon dioxide
	Silicon substrate

Photoengrave and sputter-etch top platinum electrode

6.	Platinum
	PZT
	Ti/platinum
	Silicon dioxide
	Silicon substrate

Photoengrave and wet-etch PZT layer

7.	Platinum
	PZT
	Ti/platinum
	Silicon dioxide
	Silicon substrate

Photoengrave and sputter-etch bottom Ti/pt electrode

Figure 4. Processing sequence.

Figure 5. Sol-gel process.

Mix sol-gel and hydrolyzer solutions

Filter hydrolyzed sol-gel solution through 0.2-µm filter

Apply sol-gel to wafer and spin at 1500 rpm

Bake on hotplate in air at 275°C

Repeat procedure for desired thickness

Furnace anneal in oxygen at 750°C for 30 min

about 2000 to 2500 Å. We used a standard diffusion furnace with an oxygen flow of 2 liters/min for the annealing step. It should be pointed out here that we did not attempt to optimize the ferroelectric film properties for our work, but rather were more concerned with the effects of the subsequent processing on the films after they were applied. At any rate, based on our previous experience with this process, we expected the ferroelectric films to have reasonably good electrical and mechanical properties.

The next step is to sputter-deposit the top platinum electrode. Since surface contamination of the PZT film before this step can seriously degrade the quality of the ferroelectric capacitor, the platinum should be deposited as soon as possible after the PZT films are applied. One technique that can be used to address the problem of potential surface contamination is to slightly sputter-etch the PZT film just before the actual platinum deposition. However, since we deposited the platinum immediately following the ferroelectric film anneal, we did not feel that it was necessary to do this for our work. The platinum sputtering conditions we used were 125 W for 6 min to give a platinum thickness of about 2 kÅ.

Following this platinum deposition, the top electrode was patterned and etched. To etch platinum deposited on a PZT film, some type of dry etching technique needs to be used because wet platinum etches attack the PZT film, resulting in heavy undercutting and in some cases complete pattern removal. One dry etching technique that can be used here is ion milling, which has been shown to be quite effective for this purpose. However, since an ion miller was not available to us during this work, we used a sputtering system in the etch mode to sputter-etch the platinum on the PZT. Before any actual etching was done, a number of runs were made to establish the relative sputtering etch rates of the platinum, PZT, and photoresist. Table 1 shows the etch rates for these materials at a 60-W input power. It can be observed that there is excellent etch rate selectivity between the platinum and the PZT, but that the photoresist has a relatively high sputtering rate. Nevertheless, the 1.2 µm thickness of the photoresist is more than adequate to mask the platinum electrode during the approximately 25 min required to completely etch the 2000 Å platinum layer. Figure 6 shows the etched platinum electrodes with the remaining photoresist on top. The photoresist was removed by oxygen plasma ashing for 6 min at 300 W.

At this point, the capacitors can be probed to verify proper electrical functioning. However, it is first necessary to remove a small area of PZT film to expose the bottom platinum electrode. This can be done either by mechanically abrading away the film, or by placing small drops of hydrofluoric (HF) and then 5-percent nitric acid on the film to etch it away in a suitable region such as the edge of the wafer. Figure 7 shows the hysteresis loops obtained from the 40- and 80-µm platinum electrode devices. The remanent polarization calculated from these measurements is about 25 µC/cm^2 (2 × Pr).
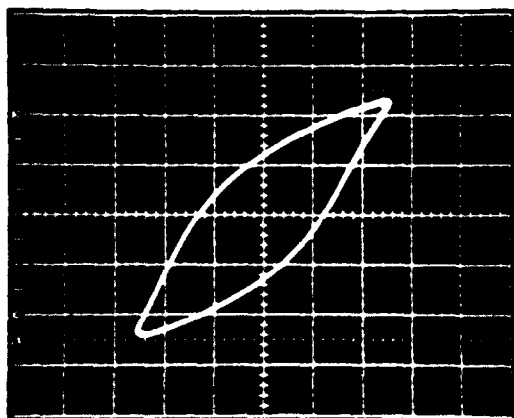
10

Table 1. Sputter-etch rates for process materials.

Material	Etch rate (Å/min)
Photoresist	300 to 500
Platinum	180
PZT	70
Silicon dioxide	50

Figure 6. Etched platinum electrodes.

(a) 80 × 80 μm
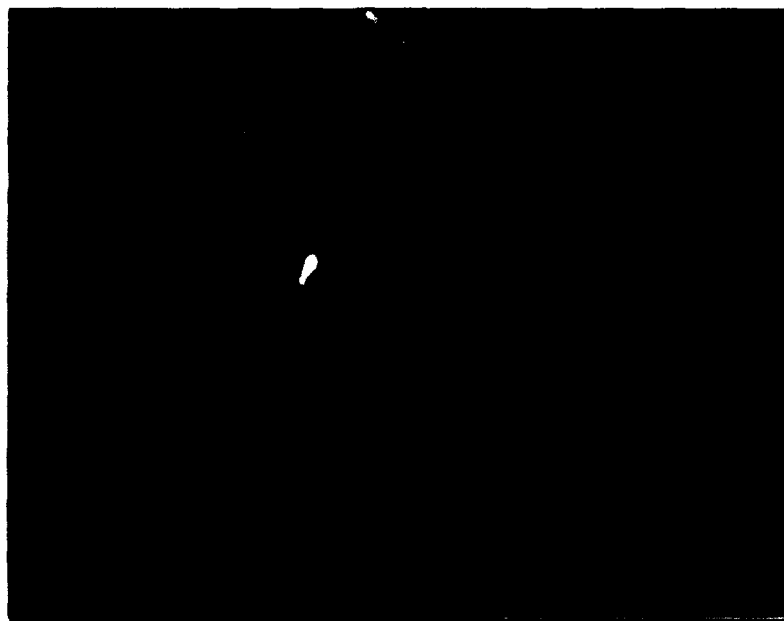
Vertical: 5 mV/div
Horizontal: 2 V/div

(b) 40 × 40 μm
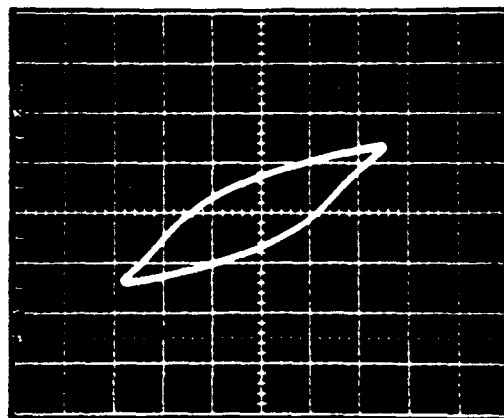
Vertical: 2 mV/div
Horizontal: 2 V/div

Figure 7. Hysteresis loops.

11

The next process steps involve the patterning and etching of the PZT film. To etch the PZT, we used a buffered HF etch consisting of seven parts of 40-percent ammonium fluoride solution to one part 48-percent HF. The sample was placed in a Teflon dish filled with the etching solution and mildly agitated during the total time in the solution. This agitation was necessary to constantly expose the PZT surface being etched to fresh etchant that had not become depleted by the etching process. The actual etching times depended upon the PZT film thickness, but an approximate etching rate of 700 Å/min was observed for the films used in our work. It was noticed that unlike the etching of silicon dioxide or other films usually encountered in integrated-circuit processing, the etching of the PZT left a film that gave the surface a dirty and uneven-looking appearance. This film was easily removed by a brief (10 to 20 s) dip in 5-percent nitric acid. The photoresist was then removed as before. Figure 8 shows the etched 40- × 40-μm PZT islands with the top platinum electrodes after the photoresist removal in the plasma asher as before. The capacitors were again characterized and found to be unchanged.

The final step in the fabrication process is the definition of the bottom electrode, by the same procedure used to etch the top platinum electrode. However, since the bottom platinum layers were somewhat thicker than the top, and because the titanium layer etches more slowly than the platinum, the time to sputter-etch the bottom electrode was increased to about 45 min. Figure 9 shows the etched bottom electrode plus the remaining photoresist. The photoresist was removed in the plasma asher as before, but this time we immersed the electrode for 5 min in Posistrip 830 maintained at a temperature of 105°C. Figure 10 shows a profile of the three-layer capacitor structure after photoresist removal. Despite the additional time required to etch the bottom electrode, the photoresist provided very good masking of the underlying capacitor structures. Figures 11 and 12 show a photomicrograph of one of the test cells and a photograph of the entire 4-in. wafer.

Figure 8. Etched PZT islands.

Figure 9. Etched bottom electrode.

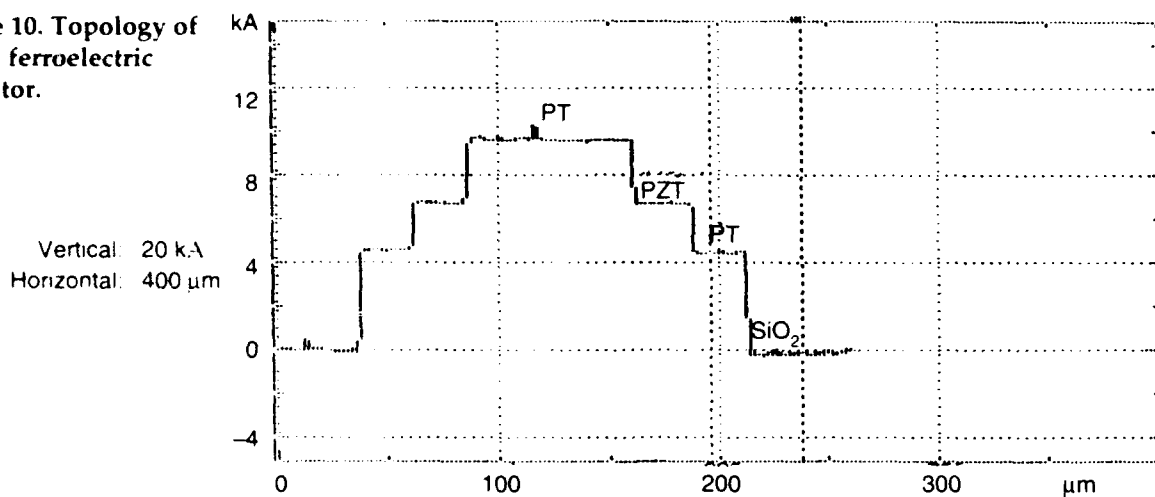Figure 10. Topology of 80-μm ferroelectric capacitor.

Vertical: 20 kÅ
Horizontal: 400 μm

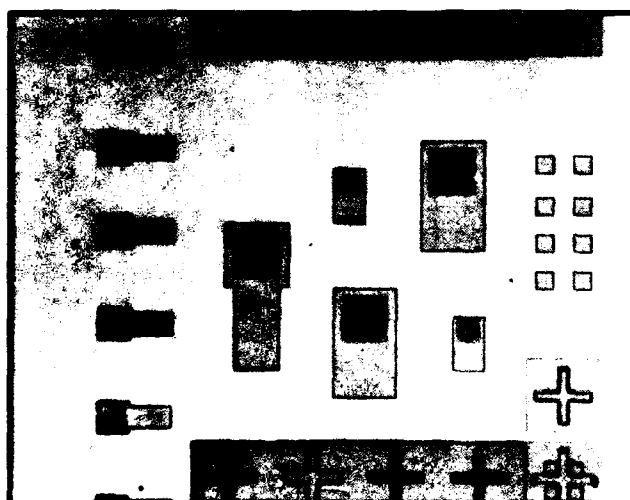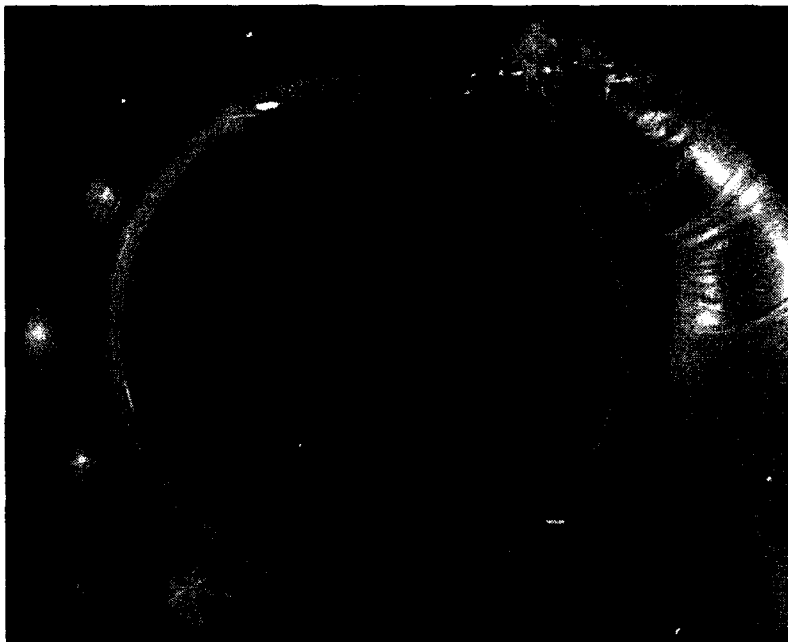Figure 11. Photomicrograph of test cell.

Figure 12. Completed wafer.

5. Device Test Results

We again point out that the ferroelectric films used in this work were not optimized to yield the best possible electrical characteristics. Nevertheless, it is worthwhile to consider the resulting electrical characteristics, if only to identify any possible degradation in the expected capacitor characteristics compared to previous measurements obtained on earlier films that saw no processing beyond shadow-mask-defined sputtered platinum electrodes. Figure 13 shows the hysteresis loops for the two different sizes of fully processed capacitors. Comparing these with the first hysteresis loops in figure 7 we see that no observable change has occurred in the devices as a result of the additional processing. A more precise analysis of the final electrical characteristics for the 80-μm device was obtained using an RT-66A ferroelectric tester. The results of these measurements are presented in figure 14. The total switched charge for the charge program hysteresis loop is observed to be 25 μC/cm^2, and the critical field about 69 kV with 5 V applied. Using the retained charge program, the 1-s retained switched charge for these devices was about 10 μC/cm^2. Details of the retained charge measurements are given in appendix A.

The measurement results presented here are similar to those obtained on earlier ferroelectric films that were prepared in the same way as the films discussed here, but with the top electrodes defined through a shadow mask so that no further processing was required to produce measurable capacitors.
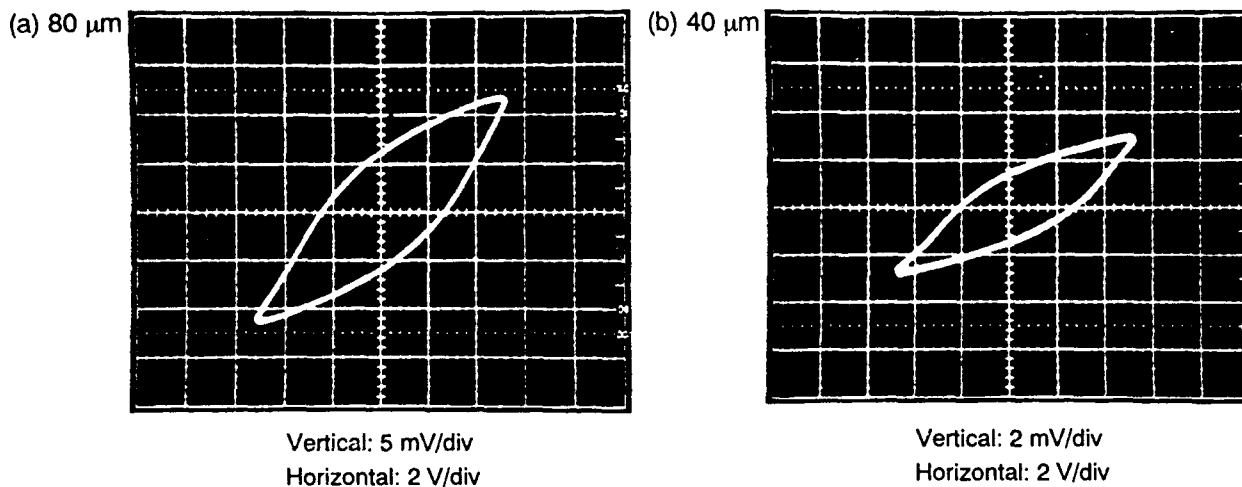
14

(a) 80 μm

Vertical: 5 mV/div
Horizontal: 2 V/div

(b) 40 μm

Vertical: 2 mV/div
Horizontal: 2 V/div

Figure 13. Hysteresis loops of fabricated capacitors.

Figure 14. RT66A results for 80-μm capacitors.

CHARGE Rev 2.0	RT-66A		Hysteresis	
Hysteresis		Virtual Ground Mode	+Ps =	24.554
	uC/cм2		+Pr =	11.537
X div = 1.250			-Pr =	-13.510
Y div = 6.2147			+Ec =	1.718
Offset = 9.637			-Ec =	-1.875
			Pulse	
			P* =	31.304
		Volts	P*r =	21.622
			P^ =	14.684
			P^r =	5.020
			C(nF)=	0.4009
			Kef =	1768
Sample:			Resistivity	
Area(cм) = 6.40E-05 Thick(u) = 0.250 Vмax = 5.000 #Pts=200			I = 2.6577E-09 -I = -1.2466E-09 R = 1.8787E+09	
Pulse = 2.400 мs Hyst = 234.333 мs Resist = 251.282 мs			-R = 4.0107E+09	
Comments:			Ry = 4.8096E+09 -Ry= 1.0267E+10	

15

6. Conclusions

We have demonstrated a process for fabricating ferroelectric capacitors in a manner that is expected to be fully compatible with CMOS integrated circuits that have been processed up to, but not including, the first aluminum metal layers. The hysteresis characteristics for the fabricated ferroelectric capacitors remained essentially unchanged through the processing sequence, and were very similar to the characteristics of capacitors produced on unprocessed ferroelectric films with the top electrodes defined by a shadow mask. The integration of the fabricated capacitors into an existing CMOS circuit would consist of preparing the CMOS wafer for the bottom platinum electrode deposition, passivating the completed capacitors using a deposited oxide or other suitable film, opening contact windows, and depositing and defining the metal layers. Work is currently in progress to define suitable passivation and metalization techniques, and to demonstrate a fully functional CMOS/ferroelectric capacitor memory element produced by the process described here.

Acknowledgments

References

1. L. H. Parke and A. F. Tasch, *Ferroelectric Materials for 64 Mb and 256 Mb DRAMs*, IEEE Circuits and Dev. Magazine, **6** (January 1990), 17.

2. F. P. Gnadinger and D. W. Bondurant, *Ferroelectrics for Nonvolatile RAMs*, IEEE Spectrum, **26** (July 1989), 30.

3. J. Scott et al., *Switching Kinetics of Lead Zirconate Titanate Submicron Thin Film Memories*, **64**, J. Appl. Phys. (1988), 787.

4. K. D. Budd, S. K. Dey, D. A. Payne, *Sol-Gel Processing of PbTiO$_3$, PZT and PLZT Thin-Films*, Proc. Br. Ceram. Soc., **36** (1985), 107.

5. S. K. Dey, K. D. Budd, D. A. Payne, *Thin-Film Ferroelectrics of PZT by Sol-Gel Processing*, IEEE Trans., **35**, Ultrason. Ferroelec. Freq. Contr. (1988), 80.

Appendix A.—Retained Charge Measurements

Acquisition Program Name: RETAIN 2.0

Data File Name: No Valid File

    Sample:
    Date of Test:

    Sample Area: 0.00006 cm
    Sample Thickness: 0.250 μm

    Vwrite: 5.000   volts   Vscale: 1.000
    Vread: 5.000   volts
    DCBias: 0.00   volts   Contacts: CLOSED
    Type Data: RETAINED SIGNAL   in Virtual Ground Mode

    Csense: 0.00470 μF   Iscale: 1.000   Ext. Iscale: 1.000
    Capacitor Measurement Amplification: 10.00000

    Number of Retention Periods: 5
    Write Pulse Width = 0.0086 milliseconds
    Read Pulse Width = 2.300 milliseconds

COMMENTS:

 RESULTS:

    Profile #5
      P*   =   15.276 μC/cm2
      P*r =   5.881 μC/cm2
    -P* = -21.622 μC/cm2
    -P*r = -15.276 μC/cm2

PROFILE:

    Retention Period# 1 =   0.30 seconds
    Retention Period# 2 =   1.00 seconds
    Retention Period# 3 =   3.00 seconds
    Retention Period# 4 = 10.00 seconds
    Retention Period# 5 = 30.00 seconds

Appendix A

RETAINED SIGNAL of Sample: for a 0.0086 ms Vwrite WRITE
pulse and a 2.300ms Vread READ pulse with a 0.00 volts
bias with contacts CLOSED after the following RETENTION periods:

Retention Period# 1 = 0.30 seconds.

        +P* [1]   =   15.383 μC/cm2
        +P*r[1]   =   5.863 μC/cm2
        −P* [1]   =   −22.788 μC/cm2
        −P*r[1]   =   −16.029 μC/cm2

Retention Period# 2 = 1.00 seconds.

        +P* [2]   =   15.096 μC/cm2
        +P*r[2]   =   5.594 μC/cm2
        −P* [2]   =   −22.626 μC/cm2
        −P*r[2]   =   −15.921 μC/cm2

Retention Period# 3 = 3.00 seconds.

        +P* [3]   =   15.150 μC/cm2
        +P*r[3]   =   5.684 μC/cm2
        −P* [3]   =   −22.411 μC/cm2
        −P*r[3]   =   −15.742 μC/cm2

Retention Period# 4 = 10.00 seconds.

        +P* [4]   =   15.258 μC/cm2
        +P*r[4]   =   5.773 μC/cm2
        −P* [4]   =   −22.071 μC/cm2
        −P*r[4]   =   −15.598 μC/cm2

Retention Period# 5 = 30.00 seconds.

        +P* [5]   =   15.276 μC/cm2
        +P*r[5]   =   5.881 μC/cm2
        −P* [5]   =   −21.622 μC/cm2
        −P*r[5]   =   −15.276 μC/cm2

Acquisition Program Name: RETAIN   2.0

Data File Name: No Valid File

    Sample:
    Date of Test:

    Sample Area: 0.00006 cm
    Sample Thickness: 0.250 μm

    Vwrite: −5.000   volts   Vscale: 1.000
    Vread: 5.000   volts
    DCBias: 0.00   volts   Contacts: CLOSED
    Type Data: RETAINED SIGNAL   in Virtual Ground Mode

    Csense: 0.00470 μF   Iscale: 1.000   Ext. Iscale: 1.000
    Capacitor Measurement Amplification: 10.00000

    Number of Retention Periods: 5
    Write Pulse Width = 0.0086 milliseconds
    Read Pulse Width = 2.300 milliseconds

COMMENTS:

 RESULTS:

    Profile #5
       P*   =   23.631 μC/cm2
       P*r =   13.841 μC/cm2
      −P*   = −21.461 μC/cm2
      −P*r = −14.128 μC/cm2

 PROFILE:

    Retention Period# 1 =   0.40 seconds
    Retention Period# 2 =   1.00 seconds
    Retention Period# 3 =   3.00 seconds
    Retention Period# 4 = 10.00 seconds
    Retention Period# 5 = 30.00 seconds

Appendix A

RETAINED SIGNAL of Sample: for a 0.0086 ms Vwrite WRITE
pulse and a 2.300ms Vread READ pulse with a 0.00 volts
bias with contacts CLOSED after the following RETENTION periods:

Retention Period# 1 = 0.40 seconds.

```
    +P*  [ 1]   =    26.302 µC/cm2
    +P*r[ 1]    =    16.459 µC/cm2
    -P*  [ 1]   =   -21.891 µC/cm2
    -P*r[ 1]    =   -14.361 µC/cm2
```

Retention Period# 2 = 1.00 seconds.

```
    +P*  [ 2]   =    24.921 µC/cm2
    +P*r[ 2]    =    15.096 µC/cm2
    -P*  [ 2]   =   -21.909 µC/cm2
    -P*r[ 2]    =   -14.379 µC/cm2
```

Retention Period# 3 = 3.00 seconds.

```
    +P*  [ 3]   =    24.455 µC/cm2
    +P*r[ 3]    =    14.684 µC/cm2
    -P*  [ 3]   =   -21.909 µC/cm2
    -P*r[ 3]    =   -14.343 µC/cm2
```

Retention Period# 4 = 10.00 seconds.

```
    +P*  [ 4]   =    24.097 µC/cm2
    +P*r[ 4]    =    14.236 µC/cm2
    -P*  [ 4]   =   -21.730 µC/cm2
    -P*r[ 4]    =   -14.289 µC/cm2
```

Retention Period# 5 = 30.00 seconds.

```
    +P*  [ 5]   =    23.631 µC/cm2
    +P*r[ 5]    =    13.841 µC/cm2
    -P*  [ 5]   =   -21.461 µC/cm2
    -P*r[ 5]    =   -14.128 µC/cm2
```

22

Distribution

Administrator
Defense Technical Information Center
Attn: DTIC-DDA (2 copies)
Cameron Station, Building 5
Alexandria, VA 22304-6145

Director
Defense Advanced Research Projects Agency
   Architect Bldg
Attn: DARPA/MTO, J. Alexander
Attn: Dir, Material Sciences
Attn: Dir, Strategic Technology Office
Attn: Dir, Technology Assessments Office
Attn: Tech Info Office
3701 N. Fairfax Dr
Arlington, VA 22203-1714

Director
Defense Communications Agency
Attn: Technical Director (B102)
National Military Command System Support
Washington, DC 20305

Director
Defense Communications Engineering Center
Attn: Code R123, Technical Library
1860 Wiehle Ave
Reston, VA 22090

Director
Defense Intelligence Agency
Attn: DS-4A2
Washington, DC 20301

Director
Defense Nuclear Agency
Attn: RAEE, LTC A. Constantine
Attn: RAEE, MAJ G. Kweder
Attn: RAEE, L. Palkuti
Attn: RAEE, L. Cohn
Attn: TITL, Tech Library
6801 Telegraph Rd
Alexandria, VA 22310-3398

Commander
Field Command Defense Nuclear Agency
Attn: FCPR
Kirtland AFB, NM 87115

Under Secretary of Defense for Research &
   Engineering
Attn: Research & Advanced Tech
Attn: Asst to Sec/Atomic Energy
Attn: Dep Under Sec/Res & Advanced Tech
Attn: Dept Asst Sec/Energy Environment &
   Safety
Attn: Dep Under Sec/Test & Evaluation
Department of Defense
Washington, DC 20301

Commander
Atmospheric Sciences Laboratory
Attn: Technical Library
White Sands Missile Range, NM 88002

Commander
CECOM R&D Tech Library
Attn: ASQNC-ELC-IS-L-R
FT Monmouth, NJ 07703-5018

Director
Night Vision & Electro-Optics Lab, LABCOM
Attn: AMSEL-TMS-IO, Information Ofc
Attn: AMSEL-SI, Electronics Team
Attn: Technical Library
FT Belvoir, VA 22060

Commander
Office of Missile Electronic Warfare
Attn: Tech & Adv Concepts Div
White Sands Missile Range, NM 88002

Director
Signals Warfare Lab, VHFS
Attn: AMSEL-RD-SW-OPI, Tac Sys Div
Warrenton, VA 22186-5000

Distribution

Commander
TRASANA
Attn: ATAA-EAC
White Sands Missile Range, NM 88002

Commander
US Army Armament Munitions & Chemical
   R&D (AMCCOM) Command
Attn: SMCAR-LCN, Nuclear & Fuze Div
Attn: SMCAR-NC, Nuclear/Chemical Surety
   GP
Attn: SMCAR-TSS, STINFO Div
Dover, NJ 07801

Commander
US Army Armament, Munitions & Chemical
   Command
Attn: AMSMC-IMF-L/Tech Library
Rock Island, IL 61299-6000

Director
US Army Ballistic Research Laboratory
Attn: SLCBR
Attn: SLCBR-AM
Attn: SLCBR-TB-VL
Attn: SLCBR-X
Aberdeen Proving Ground, MD 21005-5066

Commander
US Army Communications Command
Attn: Tech Lib
FT Huachuca, AZ 85613

Chief
US Army Communications Systems Agency
Attn: SCCM-AD-SV, Library
FT Monmouth, NJ 07703

Director
US Army Electronics Technology & Devices
   Lab, LABCOM
Attn: SLCET-D
Attn: SLCET-E
Attn: SLCET-ER
Attn: SLCET-ER-S
Attn: SLCET-I, Microelectronics

Director
US Army Electronics Technology & Devices
   Lab, LABCOM (cont'd)
Attn: SLCET-IA
FT Monmouth, NJ 07703-5601

Commander
US Army Materiel Command
Attn: AMCDE, Dir for Dev & Engr
Attn: AMCDE-R, Sys Eval & Testing
Attn: AMCNC, Nuclear-Chemical Ofc
5001 Eisenhower Ave
Alexandria, VA 22333-0001

Commander
US Army Missile Command
Attn: AMCPM-LCEX
Attn: AMCPM-MDTI
Attn: AMCPM-PE-EA
Attn: AMSMI-RGP
Attn: Army Missile RDE Lab
Attn: Tech Lib
Redstone Arsenal, AL 35898-5000

Commander
US Army Missile & Munitions Center &
   School
Attn: ATSK-CTD-F
Redstone Arsenal, AL 35809

Commander
US Army Nuclear & Chemical Agency
Attn: ATCN-W, Weapons Effects Div
Attn: Technical Library
7500 Backlick Road, Bldg 2073
Springfield, VA 22150

US Army Strategic Defense Command
Attn: CSSD-SD-YA, C. Harper
Attn: A. Kuehl
Attn: D. Stott
Attn: Library
PO Box 1500
Huntsville, AL 35807

24

Distribution

Commander
US Army Tank-Automotive Command
Attn: AMSTA-GCM-SW
Warren, MI 48397-5000

Commander
US Army Test & Evaluation Command
Attn: AMSTE-CM-F
Attn: AMSTE-EO
Attn: AMSTE-TO-O, Test Operations Div
Aberdeen Proving Ground, MD 21005-5055

Commander
White Sands Missile Range
Attn: STEWS-TE-NT
White Sands Missile Range, NM 88002

Director
Naval Research Laboratory
Attn: Code 2620, Tech Library Br
Attn: Code 2627
Attn: Code 4000, Research Dept
Attn: Code 4004
Attn: Code 5210
Attn: Code 6601
Attn: Code 6440
Attn: Code 6620, Radiation Effects
Attn: Code 6627
Attn: Code 6631, J. C. Ritter
Attn: Code 6816
Attn: Code 7701
4555 Overlook Ave, SW
Washington, DC 20375

Commander
Naval Surface Warfare Center
Attn: Code WA501, Navy Nuc Prgms Ofc
Attn: E-43, Technical Library
White Oak, MD 20910

Commander
Naval Surface Warfare Center
Attn: Code WR, Research & Technology Dept
Attn: DX-21, Library Div
Dahlgren Laboratory
Dahlgren, VA 22448

Director
Armed Forces Radiobiology Research Institute
    Defense Nuclear Agency
Attn: Technical Library
National Naval Medical Center
Bethesda, MD 20014

Director
AF Avionics Laboratory
Attn: AAT, M. Friar
Attn: DH, LTC McKenzie
Attn: DHE, H. J. Hennecke
Attn: DHM, C. Friend
Attn: TE, Electronic Technology Div
Attn: TER, Electronic Res Br
Attn: TSR, STINFO Br
Wright-Patterson AFB, OH 45433

Director
Interservice Nuclear Weapons School
Kirtland AFB, NM 87115

Director
Joint Strategic Target Planning Staff, JCS
Attn: JLTW-2
Offutt AFB
Omaha, NE 68113

Office of the Deputy Chief of Staff for Res,
    Dev, & Acq
Attn: DAMA-ARZ-D, Research Programs
Attn: DAMA-CCS-D, R&D Team
Attn: DAMA-RAX, Sys Review & Analysis
    Ofc
Attn: Dir of Army Res
Washington, DC 20310

Rome Air Development Center, AF
    Deputy for Elec Tech
Attn: ESR, W. Shedd
Hanscom Field
Bedford, MA 01731

Distribution

Dept of Energy
Attn: Asst Admin for Nuclear Energy
Attn: Div of Reactor Res & Dev
Attn: Div of Space Nuclear Systems
Washington, DC 20545

Dept of Energy
Attn: Technical Information Organization
PO Box 62
Oak Ridge, TN 37830

Dept of Energy
Albuquerque Operations
Attn: Director
PO Box 5400
Albuquerque, NM 87115

Director
Argonne National Laboratory
Attn: 9700 South Cass Ave
Argonne, IL 60439

Brookhaven National Laboratory
Associated Universities, Inc
Upton, Long Island, NY 11973

Sandia National Laboratories
Attn: Technical Library
PO Box 5800
Albuquerque, NM 87185

Director
NASA Goddard Space Flight Center
Attn: 250, Tech Info Div
Greenbelt, MD 20771

Administrator
NASA Headquarters
Attn: Ofc of Aeronautics & Space Technology
Washington, DC 20546

Director
National Security Agency
Attn: TDL
FT George G. Meade, MD 20755

US Department of Commerce
Attn: Assistant Secretary for Science &
   Technology
Washington, DC 20230

Engineering Societies Library
Attn: Acquisitions Department
345 East 47th St.
New York, NY 10017

Harris Corporation Electronic Systems Center
Attn: MS 101/4825, W. Abare
PO Box 37
Melbourne, FL 32392

Honeywell Incorporated
Government & Aeronautical Products Div
Attn: J. Schrankler
2600 Ridgeway Parkway
Minneapolis, MN 55413

Jet Propulsion Laboratory
California Institute of Technology
Attn: D. J. Nichols, T-1180
Attn: Technical Library
4800 Oak Grove Drive
Pasadena, CA 91103

Kaman Tempo
Attn: C. Fore
2560 Huntington Ave, Suite 506
Alexandria, VA 22303

Mission Research Corp
Attn: E. Enlow
Attn: R. Pease
1720 Randolph Rd, SE
Albuquerque, NM 87106

Mitre Corporation
Attn: Library
Attn: M. Fitzgerald
PO Box 208
Bedford, MA 01730

26

Distribution

Teledyne Brown Engineering
Attn: A. Fenelly
Cummings Research Park
Huntsville, AL 35807

US Army Laboratory Command
Attn: AMSLC-DL, Dir Corp Labs

Installation Support Activity
Attn: SLCIS-CC-IP, Legal Office

USAISC
Attn: AMSLC-IM-VA, Admin Ser Br
Attn: AMSLC-IM-VP, Tech Pub Br
  (2 copies)

Harry Diamond Laboratories
Attn: Laboratory Directors
Attn: SLCHD-SD-TL, Library (3 copies)
Attn: SLCHD-SD-TL, Library (Woodbridge)
Attn: SLCHD-NW, Director
Attn: SLCHD-NW, J. M. McGarrity
Attn: SLCHD-NW-E, Deputy Director
Attn: SLCHD-NW-EH, Chief
Attn: SLCHD-NW-EP, Chief
Attn: SLCHD-NW-ES, Chief
Attn: SLCHD-NW-P, Chief
Attn: SLCHD-NW-RF, Chief

Harry Diamond Laboratories (cont'd)
Attn: SLCHD-NW-RP, Chief
Attn: SLCHD-NW-RS, Chief
Attn: SLCHD-NW-TN, Chief
Attn: SLCHD-NW-TS, Chief
Attn: SLCHD-D, R. Gilbert
Attn: SLCHD-NW-EP, J. R. Miletta
Attn: SLCHD-NW-P, D. Davis
Attn: SLCHD-NW-RP, J. Benedetto
Attn: SLCHD-NW-RP, K. W. Bennett
Attn: SLCHD-NW-RP, T. V. Blomquist
Attn: SLCHD-NW-RP, H. Boesch
Attn: SLCHD-NW-RP, B. Geil
Attn: SLCHD-NW-RP, T. Griffin
Attn: SLCHD-NW-RP, A. J. Lelis
Attn: SLCHD-NW-RP, J. McCullen
Attn: SLCHD-NW-RP, B. McLean
Attn: SLCHD-NW-RP, T. Mermagen
Attn: SLCHD-NW-RP, R. B. Reams
  (5 copies)
Attn: SLCHD-NW-RS, H. Brandt
Attn: SLCHD-NW-TS, H. Eisen
Attn: SLCHD-TA-ES, R. Goodman
Attn: SLCHD-NW-RP, B. J. Rod (20 copies)

27